



ISSN 1600-5368

Crystal structure of magnesium selenate heptahydrate, $\text{MgSeO}_4 \cdot 7\text{H}_2\text{O}$, from neutron time-of-flight data

A. Dominic Fortes^{a,b,*} and Matthias J. Gutmann^cReceived 6 August 2014
Accepted 18 August 2014^aDepartment of Earth Sciences, University College London, Gower Street, London WC1E 6BT, England, ^bDepartment of Earth and Planetary Sciences, Birkbeck, University of London, Malet Street, London WC1E 7HX, England, and ^cISIS Facility, STFC Rutherford Appleton Laboratory, Harwell Science and Innovation Campus, Chilton, Didcot, Oxfordshire OX11 0QX, England. *Correspondence e-mail: andrew.fortes@ucl.ac.uk

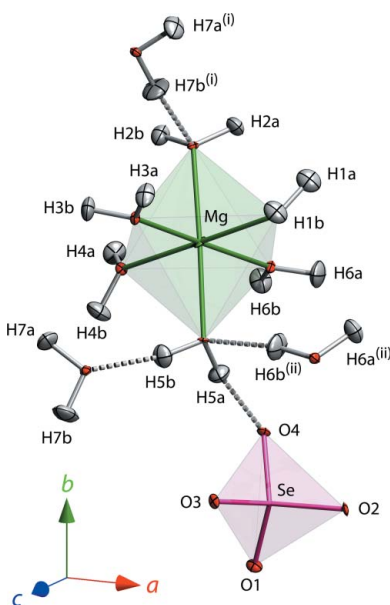
Edited by M. Weil, Vienna University of Technology, Austria

Keywords: crystal structure; magnesium selenate heptahydrate; neutron Laue diffraction; hydrogen bonding**CCDC reference:** 1019812**Supporting information:** this article has supporting information at journals.iucr.org/e

$\text{MgSeO}_4 \cdot 7\text{H}_2\text{O}$ is isostructural with the analogous sulfate, $\text{MgSO}_4 \cdot 7\text{H}_2\text{O}$, consisting of isolated $[\text{Mg}(\text{H}_2\text{O})_6]^{2+}$ octahedra and $[\text{SeO}_4]^{2-}$ tetrahedra, linked by $\text{O}-\text{H} \cdots \text{O}$ hydrogen bonds, with a single interstitial lattice water molecule. As in the sulfate, the $[\text{Mg}(\text{H}_2\text{O})_6]^{2+}$ coordination octahedron is elongated along one axis due to the tetrahedral coordination of the two apical water molecules; these have $\text{Mg}-\text{O}$ distances of $\sim 2.10 \text{ \AA}$, whereas the remaining four trigonally coordinated water molecules have $\text{Mg}-\text{O}$ distances of $\sim 2.05 \text{ \AA}$. The mean $\text{Se}-\text{O}$ bond length is 1.641 \AA and is in excellent agreement with other selenates. The unit-cell volume of $\text{MgSeO}_4 \cdot 7\text{H}_2\text{O}$ at 10 K is 4.1% larger than that of the sulfate at 2 K, although this is not uniform; the greater part of the expansion is along the a axis of the crystal.

1. Chemical context

Since their discovery almost two hundred years ago, the heptahydrates of divalent metal selenates have received scant attention. This is in stark contrast with the $M^{2+}\text{SeO}_4$ hexahydrates, which have been extensively characterized, including studies of their morphology and optical properties (Topsøe & Christiansen, 1874), their crystal structures (Stadnicka *et al.*, 1988; Kolitsch, 2002), their formation of isomorphous solution series (*e.g.*, Ojkova *et al.*, 1990; Stoilova *et al.*, 1995) and their dehydration properties (Nabar & Paralkar, 1975; Stoilova & Koleva, 1995). In part this may be due to the fact that the heptahydrates must be prepared at lower temperatures. Nevertheless, it is striking that the only information concerning their crystal structures, namely their apparent isomorphism with the $M^{2+}\text{SO}_4$ heptahydrates, has remained largely unaltered since the observations made prior to 1830 by Berzelius and his student Mitscherlich, which is that $\text{MgSeO}_4 \cdot 7\text{H}_2\text{O}$ forms deliquescent four-sided prismatic crystals below 288 K (*e.g.*, Berzelius, 1818, 1829). The only known goniometric data relate to $\text{FeSeO}_4 \cdot 7\text{H}_2\text{O}$ and $\text{CoSeO}_4 \cdot 7\text{H}_2\text{O}$ (Wohlwill, 1860; Topsøe, 1870; Tutton, 1918), which are isomorphous with the monoclinic series of $M^{2+}\text{SO}_4$ heptahydrates. It is worth stating that $\text{MgMoO}_4 \cdot 5\text{H}_2\text{O}$ is isomorphous with both the sulfate, chromate and selenate analogues but is not isostructural with them [Bars *et al.*, 1977; see also Lima-de-Faria *et al.* (1990) for further discussion of these nomenclature], so the occurrence of $\text{MgSeO}_4 \cdot 7\text{H}_2\text{O}$ as acicular rhombic prisms is no guarantee that it is isostructural with the sulfate salt. Additional confusion arises from conflicting observations of the $\text{MgSeO}_4-\text{H}_2\text{O}$ binary phase diagram (Meyer & Aulich, 1928; Klein, 1940), including our own recent



OPEN ACCESS

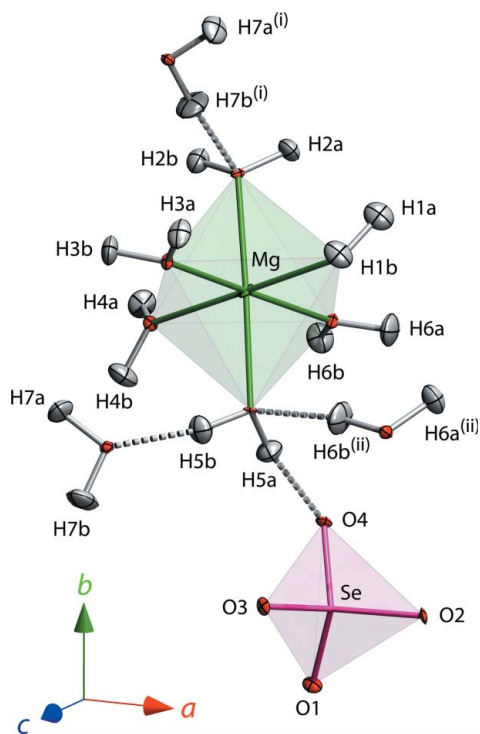


Figure 1

Asymmetric unit of $\text{MgSeO}_4 \cdot 7\text{H}_2\text{O}$ with anisotropic displacement ellipsoids drawn at the 50% probability level (75% for Mg and the selenate O atoms to aid visibility). Dashed rods indicate hydrogen bonds. The superscripts (i) and (ii) denote, respectively, the symmetry operations $[1 - x, \frac{1}{2} + y, \frac{3}{2} - z]$ and $[\frac{3}{2} - x, 1 - y, \frac{1}{2} + z]$.

discovery of hitherto unknown hydrates (containing $9\text{H}_2\text{O}$ and $11\text{H}_2\text{O}$) below 273 K (Fortes, 2014).

As part of a wider study into low-temperature crystal hydrates of MgSeO_4 and related compounds (Fortes *et al.*, 2013) we synthesised the title compound and carried out a single-crystal neutron diffraction experiment in order to determine its structure.

2. Structural commentary

The crystal structure (Fig. 1) is isostructural with that of the sulfate, having isolated $[\text{Mg}(\text{H}_2\text{O})_6]^{2+}$ octahedra and $[\text{SeO}_4]^{2-}$ tetrahedra linked by a framework of moderately strong hydrogen bonds ($\text{H} \cdots \text{O}$ from 1.692 to 1.946 Å; Table 1). The seventh water molecule is coordinated to neither Mg nor Se, occupying a ‘void’ between the polyhedral ions and donating comparatively weak (*i.e.*, long and non-linear) hydrogen bonds (Fig. 2, Table 1). The $[\text{Mg}(\text{H}_2\text{O})_6]^{2+}$ octahedron is slightly elongated along the $\text{OW2} - \text{Mg} - \text{OW5}$ axis, the respective $\text{Mg}-\text{O}$ distances being 2.101 Å (average) compared with 2.046 Å (average) for the other four ‘equatorial’ water molecules (Table 2). This distortion was also noted in the sulfate by Baur (1964) and is manifested in subsequent neutron single-crystal and powder diffraction studies (Ferraris *et al.*, 1973; Fortes *et al.*, 2006). The difference is due to the tetrahedral coordination of OW2 and OW5 ; both of these water molecules (in addition to being Mg-coordin-

Table 1

Hydrogen-bond geometry (Å, °).

$D-\text{H} \cdots A$	$D-\text{H}$	$\text{H} \cdots A$	$D \cdots A$	$D-\text{H} \cdots A$
$\text{OW1}-\text{H1A} \cdots \text{O3}^{\text{i}}$	0.969 (16)	1.692 (16)	2.659 (9)	175.4 (13)
$\text{OW1}-\text{H1B} \cdots \text{O4}^{\text{ii}}$	0.968 (16)	1.757 (15)	2.724 (9)	175.1 (11)
$\text{OW2}-\text{H2A} \cdots \text{O2}^{\text{i}}$	0.983 (14)	1.781 (15)	2.757 (9)	171.0 (11)
$\text{OW2}-\text{H2B} \cdots \text{O4}^{\text{iii}}$	0.984 (11)	1.753 (11)	2.732 (7)	172.4 (10)
$\text{OW3}-\text{H3A} \cdots \text{O2}^{\text{ii}}$	0.976 (13)	1.889 (13)	2.861 (8)	174.5 (12)
$\text{OW3}-\text{H3B} \cdots \text{O3}^{\text{iv}}$	0.985 (9)	1.708 (9)	2.692 (6)	177.4 (14)
$\text{OW4}-\text{H4A} \cdots \text{O1}^{\text{iii}}$	0.976 (14)	1.720 (15)	2.688 (9)	170.9 (11)
$\text{OW4}-\text{H4B} \cdots \text{O2}^{\text{v}}$	0.964 (13)	1.927 (11)	2.861 (7)	162.3 (15)
$\text{OW5}-\text{H5A} \cdots \text{O4}$	0.976 (14)	1.874 (14)	2.839 (8)	169.6 (10)
$\text{OW5}-\text{H5B} \cdots \text{OW7}$	0.967 (15)	1.786 (14)	2.742 (9)	169.4 (10)
$\text{OW6}-\text{H6A} \cdots \text{OW5}^{\text{i}}$	0.976 (10)	1.875 (10)	2.841 (6)	170.3 (12)
$\text{OW6}-\text{H6B} \cdots \text{OW7}^{\text{vi}}$	0.982 (14)	1.809 (13)	2.787 (8)	173.4 (11)
$\text{OW7}-\text{H7A} \cdots \text{O1}^{\text{iv}}$	0.973 (10)	1.858 (12)	2.790 (7)	159.5 (14)
$\text{OW7}-\text{H7B} \cdots \text{OW2}^{\text{vii}}$	0.955 (13)	1.946 (16)	2.866 (8)	161.2 (15)

Symmetry codes: (i) $-x + \frac{3}{2}, -y + 1, z - \frac{1}{2}$; (ii) $-x + \frac{3}{2}, -y + 1, z + \frac{1}{2}$; (iii) $-x + 1, y + \frac{1}{2}, -z + \frac{1}{2}$; (iv) $-x + 1, y + \frac{1}{2}, -z + \frac{3}{2}$; (v) $x - \frac{1}{2}, -y + \frac{1}{2}, -z + 1$; (vi) $x, y, z - 1$; (vii) $-x + 1, y - \frac{1}{2}, -z + \frac{3}{2}$.

Table 2

Selected bond lengths (Å).

$\text{Se1}-\text{O1}$	1.630 (6)	$\text{Mg1}-\text{OW1}$	2.045 (6)
$\text{Se1}-\text{O3}$	1.631 (8)	$\text{Mg1}-\text{OW3}$	2.046 (10)
$\text{Se1}-\text{O2}$	1.642 (4)	$\text{Mg1}-\text{OW6}$	2.058 (9)
$\text{Se1}-\text{O4}$	1.661 (7)	$\text{Mg1}-\text{OW5}$	2.097 (8)
$\text{Mg1}-\text{OW4}$	2.037 (6)	$\text{Mg1}-\text{OW2}$	2.104 (8)

ated) donate two hydrogen bonds and accept one hydrogen bond, from OW7 and OW6 respectively. The four ‘equatorial’ water molecules donate but do not accept any hydrogen bonds. In the sulfate at 2 K (Fortes *et al.*, 2006), the average equatorial $\text{Mg}-\text{O}$ distances were found to be 2.029 Å and the average axial $\text{Mg}-\text{O}$ distances to be 2.100 Å (2.056 and

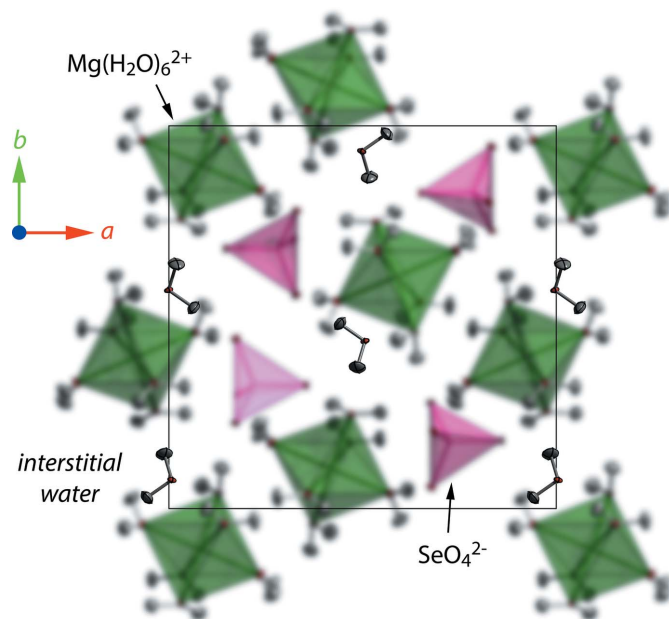


Figure 2

Packing of the polyhedra and interstitial water in $\text{MgSeO}_4 \cdot 7\text{H}_2\text{O}$ viewed down the c -axis. The polyhedral ions have been blurred in order to emphasize the location of the interstitial water molecules.

2.102 Å at room temperature; Ferraris *et al.*, 1973; Calleri *et al.*, 1984).

The [SeO₄]²⁻ tetrahedron exhibits a similar property in that the bond lengths are influenced by the hydrogen-bond coordination. Two of the oxygen atoms (O1 and O3) accept two hydrogen bonds and have mean Se–O bond lengths of 1.631 Å, whereas the other two oxygen atoms (O2 and O4) accept three hydrogen bonds and have a mean Se–O bond length of 1.652 Å. This distinction is not readily apparent in any of the data pertaining to the sulfate, but it is worth observing that the neutron scattering cross-section of selenium is almost three times greater than that of sulfur so our result should be considered more accurate. The mean Se–O bond length of 1.641 Å is in excellent agreement with other similar high-precision analyses of selenate crystals (Kolitsch, 2001, 2002; Weil & Bonneau, 2014).

Overall, the unit-cell volume of the selenate at 10 K is 4.1% larger than the sulfate analogue (deuterated) at 2 K. This expansion is not isotropic, however, with the greatest proportion being along the *a* axis of the crystal. We find that the *a* axis is 2.7% longer, the *b* axis 1.0% longer, and the *c* axis 0.3% longer in the selenate than the sulfate. It is not readily apparent from examination of the structure why this should be so. The magnitude of the volumetric strain is virtually identical to that found in MgSeO₄·11H₂O (4.1% larger than the sulfate analogue; Fortes, 2014) and somewhat less than is observed in, for example, CuSeO₄·5H₂O (5.1% larger than the equivalent sulfate; Kolitsch, 2001) or MgSeO₄·6H₂O (5.2%; Kolitsch, 2002).

3. Synthesis and crystallization

In our initial attempts to make MgSeO₄ we employed the widely cited method of reacting basic Mg-carbonate with aqueous selenic acid (*e.g.*, Stoilova & Koleva, 1995), but this was found to leave a substantial amount of acid in solution, giving a pink-coloured viscous liquid with a sour odour, which yielded an intimate mixture of MgSeO₄·6H₂O and Mg(HSeO₃)₂·4H₂O crystals (*cf.*, Kolitsch, 2002; Mička *et al.*, 1996) even after repeated re-crystallization and treatment with aqueous H₂O₂. Consequently, we prepared an aqueous solution of magnesium selenate by stirring MgO into a solution of H₂SeO₄ (Sigma–Aldrich 481513, 40%_wt diluted further in its own weight of distilled water) heated to 340 K. This reaction is much less dramatic than is the case when Mg-carbonate is used and the only clear indication that it has run to completion is the pH of the solution, which changed from 0.11 to 8.80. After a period of evaporation in the open air, the solution precipitates cm-sized crystals of MgSeO₄·6H₂O. After a further round of recrystallization from distilled water the phase purity of the hexahydrate was verified both by X-ray powder diffraction and Raman spectroscopy.

Finally, crystalline MgSeO₄·6H₂O was dissolved in distilled water to a concentration of 35%_wt MgSeO₄ at 333 K, and this liquid was left to evaporate in a refrigerated workshop at 269 K. After two days, slender prismatic crystals indis-

Table 3
Experimental details.

Crystal data	
Chemical formula	[Mg(H ₂ O) ₆](SeO ₄)(H ₂ O)
<i>M_r</i>	293.38
Crystal system, space group	Orthorhombic, <i>P</i> 2 ₁ 2 ₁ 2 ₁
Temperature (K)	10
<i>a</i> , <i>b</i> , <i>c</i> (Å)	12.234 (4), 12.020 (4), 6.809 (3)
<i>V</i> (Å ³)	1001.3 (6)
<i>Z</i>	4
Radiation type	Neutron, λ = 0.48–7.0 Å
μ (mm ⁻¹)	0.48 + 0.0036 * λ
Crystal size (mm)	1.00 × 1.00 × 4.00
Data collection	
Diffractometer	SXD diffractometer
Absorption correction	Numerical. The linear absorption coefficient is wavelength dependent and is calculated as: μ = 0.4823 + 0.0036 * λ [mm ⁻¹] as determined by Gaussian integration in <i>SXD2001</i> (Gutmann, 2005)
No. of measured, independent and observed [<i>I</i> > 2σ(<i>I</i>)] reflections	4337, 4337, 4337
Refinement	
<i>R</i> [<i>F</i> ² > 2σ(<i>F</i> ²)], <i>wR</i> (<i>F</i> ²), <i>S</i>	0.072, 0.197, 1.08
No. of reflections	4337
No. of parameters	252
H-atom treatment	All H-atom parameters refined w = 1/[σ ² (<i>F_o</i> ²) + (0.1399 <i>P</i>) ² + 21.2928 <i>P</i>] where <i>P</i> = (<i>F_o</i> ² + 2 <i>F_c</i> ²)/3
Δρ _{max} , Δρ _{min} (fermi Å ⁻³)	2.06, -1.72
Absolute structure	All <i>f</i> ' are zero, so absolute structure could not be determined

Computer programs: *SXD2001* (Gutmann, 2005), *SHELXS2014* and *SHELXL2014* (Grüne *et al.*, 2014), *DIAMOND* (Putz & Brandenburg, 2006) and *pubCIF* (Westrip, 2010).

tinguishable in habit from MgSO₄·7H₂O, appeared. One of these was removed from the liquid, dried on filter paper and cut into a pair of fragments each with dimensions 1 x 1 x 4 mm. The two fragments were placed side-by-side in an aluminium foil pouch suspended inside a standard thin-walled vanadium sample can (6 mm inner diameter). The lid of the can was sealed with indium wire and was then transported to the ISIS neutron source immersed in liquid nitrogen.

The sample can was screwed onto a standard centre stick and inserted into a pre-cooled Closed-Cycle Refrigerator (CCR) already mounted on the SXD beam-line (Keen *et al.*, 2006). Initial data collection as the sample was cooled from 200 K down to 10 K revealed strong reflections from both crystals that could be indexed with an orthorhombic unit cell of similar shape but roughly 4% larger than that of MgSO₄·7H₂O. After cooling to 10 K data were collected with the crystals in four discrete orientations with respect to the incident beam, optimizing the coverage of reciprocal space, with integration times of 1600 μAhr each (roughly 10 h per frame at typical ISIS beam intensity). The peaks were indexed and integrated using the instrument software, *SXD2001* (Gutmann, 2005) and exported in a format suitable for analysis using *SHELX2014* (Sheldrick, 2008; Grüne *et al.*, 2014).

Upon completion of the experiment, crystals of the title compound that had been stored in a glass vial at 253 K for ten days were analysed by means of X-ray powder diffraction. This measurement, carried out on a custom Peltier cold stage (Wood *et al.*, 2012) at 253 K, revealed that the heptahydrate had transformed completely to the newly reported $\text{MgSeO}_4 \cdot 9\text{H}_2\text{O}$ (Fortes, 2014), thus providing some initial insight into the relative stability of the two compounds.

4. Refinement

Crystal data, data collection and structure refinement details are summarized in Table 3. Structure refinement with *SHELXL* using the model obtained at 2 K for the deuterated MgSO_4 analogue (Fortes *et al.*, 2006) based on earlier work (Baur, 1964; Ferraris *et al.*, 1973; Calleri *et al.*, 1984) yielded a good fit with no density residuals larger than 4.5% of the nuclear scattering density due to a hydrogen atom. No restraints were used and all anisotropic temperature factors were refined independently.

Acknowledgements

The authors thank the STFC ISIS facility for beam-time access and ADF acknowledges financial support from STFC, grant Nos. PP/E006515/1 and ST/K000934/1.

References

- Bars, O., Le Marouille, J.-Y. & Grandjean, D. (1977). *Acta Cryst.* **B33**, 1155–1157.
- Baur, W. H. (1964). *Acta Cryst.* **17**, 1361–1369.
- Berzelius, J. (1818). *J. Chem. Phys.* **23**, 430–484.
- Berzelius, J. (1829). *Jahres-Bericht über die Fortschritte der Physischen Wissenschaften*. Tübingen.
- Calleri, M., Gavetti, A., Ivaldi, G. & Rubbo, M. (1984). *Acta Cryst.* **B40**, 218–222.
- Ferraris, G., Jones, D. W. & Yerkess, J. (1973). *J. Chem. Soc. Dalton Trans.* **8**, 816–821.
- Fortes, A. D. (2014). *Powder Diffr.* Submitted.
- Fortes, A. D., Wood, I. G., Alfredsson, M., Vočadlo, L. & Knight, K. S. (2006). *Eur. J. Min.* **18**, 449–462.
- Fortes, A. D., Wood, I. G. & Gutmann, M. J. (2013). *Acta Cryst.* **C69**, 324–329.
- Gruene, T., Hahn, H. W., Luebben, A. V., Meilleur, F. & Sheldrick, G. M. (2014). *J. Appl. Cryst.* **47**, 462–466.
- Gutmann, M. J. (2005). *SXD2001*. ISIS Facility, Rutherford Appleton Laboratory, Oxfordshire, England.
- Keen, D. A., Gutmann, M. J. & Wilson, C. C. (2006). *J. Appl. Cryst.* **39**, 714–722.
- Klein, A. (1940). *Ann. Chim.* **14**, 263–317.
- Kolitsch, U. (2001). *Acta Cryst.* **E57**, i104–i105.
- Kolitsch, U. (2002). *Acta Cryst.* **E58**, i3–i5.
- Lima-de-Faria, J., Hellner, E., Liebau, F., Makovicky, E. & Parthé, E. (1990). *Acta Cryst.* **A46**, 1–11.
- Meyer, J. & Aulich, W. (1928). *Z. Anorg. Allg. Chem.* **172**, 321–343.
- Mička, Z., Němec, I. & Vojtíšek, P. (1996). *J. Solid State Chem.* **122**, 338–342.
- Nabar, M. A. & Paralkar, S. V. (1975). *Thermochim. Acta*, **13**, 93–95.
- Ojkova, T., Balarew, C. & Staneva, D. (1990). *Z. Anorg. Allg. Chem.* **584**, 217–224.
- Putz, H. & Brandenburg, K. (2006). *DIAMOND*. Crystal Impact GbR, Bonn, Germany.
- Sheldrick, G. M. (2008). *Acta Cryst.* **A64**, 112–122.
- Stadnicka, K., Glazer, A. M. & Koralewski, M. (1988). *Acta Cryst.* **B44**, 356–361.
- Stoilova, D. & Koleva, V. (1995). *Thermochim. Acta*, **255**, 33–38.
- Stoilova, D., Ojkova, T. & Staneva, D. (1995). *Cryst. Res. Technol.* **30**, 3–7.
- Topsøe, H. (1870). *Krystallografisk-kemiske Undersøgelser over de selensure salte*. Dissertation, København, Denmark.
- Topsøe, H. & Christiansen, C. (1874). *Ann. Chim. Phys. 5e Série*, **1**, 5–99.
- Tutton, A. E. H. (1918). *Proc. Roy. Soc. London. A*, **94**, 352–361.
- Weil, M. & Bonneau, B. (2014). *Acta Cryst.* **E70**, 54–57.
- Westrip, S. P. (2010). *J. Appl. Cryst.* **43**, 920–925.
- Wohllwill, E. (1860). *Über isomorphe Mischungen der selensauren Salze*. Dissertation, Georg-August Universität Göttingen, Germany.
- Wood, I. G., Hughes, N. J., Browning, F. & Fortes, A. D. (2012). *J. Appl. Cryst.* **45**, 608–610.

supporting information

Acta Cryst. (2014). E70, 134-137 [doi:10.1107/S1600536814018698]

Crystal structure of magnesium selenate heptahydrate, $\text{MgSeO}_4 \cdot 7\text{H}_2\text{O}$, from neutron time-of-flight data

A. Dominic Fortes and Matthias J. Gutmann

Computing details

Data collection: *SXD2001* (Gutmann, 2005); cell refinement: *SXD2001* (Gutmann, 2005); data reduction: *SXD2001* (Gutmann, 2005); program(s) used to solve structure: *SHELXS2014* (Gruene *et al.*, 2014); program(s) used to refine structure: *SHELXL2014* (Gruene *et al.*, 2014); molecular graphics: *DIAMOND* (Putz & Brandenburg, 2006); software used to prepare material for publication: *publCIF* (Westrip, 2010).

Hexaaquamagnesium(II) selenate monohydrate

Crystal data

$[\text{Mg}(\text{H}_2\text{O})_6](\text{SeO}_4)(\text{H}_2\text{O})$

$M_r = 293.38$

Orthorhombic, $P2_12_12_1$

$a = 12.234$ (4) Å

$b = 12.020$ (4) Å

$c = 6.809$ (3) Å

$V = 1001.3$ (6) Å³

$Z = 4$

$F(000) = 592$

$D_x = 1.946$ Mg m⁻³

Neutron radiation, $\lambda = 0.48\text{--}7.0$ Å

Cell parameters from 550 reflections

$\mu = 0.48 + 0.0036 * \lambda$ mm⁻¹

$T = 10$ K

Rhomboid, colourless

$4.00 \times 1.00 \times 1.00$ mm

Data collection

SXD

diffractometer

Radiation source: ISIS neutron spallation source

time-of-flight LAUE diffraction scans

Absorption correction: numerical

The linear absorption coefficient is wavelength dependent and is calculated as: $\mu = 0.4823 + 0.0036 * \lambda$ [mm⁻¹] as determined by Gaussian integration in *SXD2001* (Gutmann, 2005)

$T_{\min} = ?$, $T_{\max} = ?$

4337 measured reflections

4337 independent reflections

4337 reflections with $I > 2\sigma(I)$

$\theta_{\max} = 84.5^\circ$, $\theta_{\min} = 0.001^\circ$

$h = -32 \rightarrow 30$

$k = -31 \rightarrow 20$

$l = -11 \rightarrow 6$

Refinement

Refinement on F^2

Least-squares matrix: full

$R[F^2 > 2\sigma(F^2)] = 0.072$

$wR(F^2) = 0.197$

$S = 1.08$

4337 reflections

252 parameters

0 restraints

Primary atom site location: structure-invariant direct methods

Hydrogen site location: difference Fourier map

All H-atom parameters refined

$w = 1/[\sigma^2(F_o^2) + (0.1399P)^2 + 21.2928P]$

where $P = (F_o^2 + 2F_c^2)/3$

$(\Delta/\sigma)_{\max} < 0.001$

$\Delta\rho_{\max} = 2.06$ e Å⁻³

$\Delta\rho_{\min} = -1.72$ e Å⁻³

Extinction correction: *SHELXL2014* (Gruene et al., 2014), $F_c^* = kFc[1 + 0.001 \times Fc^2 \lambda^3 / \sin(2\theta)]^{-1/4}$
 Extinction coefficient: 0.0026 (3)

Absolute structure: All f'' are zero, so absolute structure could not be determined

Special details

Experimental. For peak integration a local UB matrix refined for each frame, using approximately 50 reflections from each of the 11 detectors. Hence `_cell_measurement_reflns_used` 550 For final cell dimensions a weighted average of all local cells was calculated Because of the nature of the experiment, it is not possible to give values of `theta_min` and `theta_max` for the cell determination. The same applies for the wavelength used for the experiment. The range of wavelengths used was 0.48–7.0 Angstroms, BUT the bulk of the diffraction information is obtained from wavelengths in the range 0.7–2.5 Angstroms. The data collection procedures on the SXD instrument used for the single-crystal neutron data collection are most recently summarized in the Appendix to the following paper Wilson, C. C. (1997). *J. Mol. Struct.* 405, 207–217

Geometry. All e.s.d.s (except the e.s.d. in the dihedral angle between two l.s. planes) are estimated using the full covariance matrix. The cell e.s.d.s are taken into account individually in the estimation of e.s.d.s in distances, angles and torsion angles; correlations between e.s.d.s in cell parameters are only used when they are defined by crystal symmetry. An approximate (isotropic) treatment of cell e.s.d.s is used for estimating e.s.d.s involving l.s. planes.

Refinement. The variable wavelength nature of the data collection procedure means that sensible values of `_diffn_reflns_theta_min` & `_diffn_reflns_theta_max` cannot be given instead the following limits are given `_diffn_reflns_sin(theta)/lambda_min` 0.06 `_diffn_reflns_sin(theta)/lambda_max` 1.38 `_refine_diff_density_max/min` is given in Fermi per angstrom cubed not electrons per angstrom cubed. Another way to consider the `_refine_diff_density_` is as a percentage of the scattering density of a given atom: `_refine_diff_density_max` = 4.5% of hydrogen `_refine_diff_density_min` = -3.8% of hydrogen Refinement of F^2 against ALL reflections. The weighted R -factor wR and goodness of fit S are based on F^2 , conventional R -factors R are based on F , with F set to zero for negative F^2 . The threshold expression of $F^2 > \sigma(F^2)$ is used only for calculating R -factors(gt) etc. and is not relevant to the choice of reflections for refinement. R -factors based on F^2 are statistically about twice as large as those based on F , and R -factors based on ALL data will be even larger. For comparison, the calculated R -factor based on F is 0.0578 for the 1606 unique reflections obtained after merging to generate the Fourier map.

Fractional atomic coordinates and isotropic or equivalent isotropic displacement parameters (\AA^2)

	<i>x</i>	<i>y</i>	<i>z</i>	$U_{\text{iso}}^*/U_{\text{eq}}$
Se1	0.72001 (19)	0.1764 (3)	0.4966 (7)	0.0005 (6)
O1	0.6727 (3)	0.0565 (4)	0.4240 (10)	0.0045 (10)
O2	0.8540 (3)	0.1781 (4)	0.4840 (10)	0.0039 (10)
O3	0.6788 (3)	0.2016 (4)	0.7201 (10)	0.0032 (9)
O4	0.6714 (3)	0.2769 (4)	0.3540 (10)	0.0037 (10)
Mg1	0.5841 (3)	0.6050 (4)	0.4601 (11)	0.0028 (11)
OW1	0.7361 (3)	0.6719 (5)	0.5016 (11)	0.0053 (10)
OW2	0.5312 (3)	0.7470 (4)	0.3064 (10)	0.0046 (10)
OW3	0.5370 (3)	0.6718 (5)	0.7231 (10)	0.0052 (10)
OW4	0.4319 (3)	0.5399 (4)	0.4219 (10)	0.0049 (11)
OW5	0.6304 (3)	0.4595 (4)	0.6082 (10)	0.0042 (10)
OW6	0.6434 (3)	0.5384 (4)	0.2028 (11)	0.0059 (11)
OW7	0.5042 (3)	0.4328 (4)	0.9377 (11)	0.0048 (10)
H1A	0.7663 (8)	0.7214 (10)	0.403 (2)	0.019 (2)
H1B	0.7660 (8)	0.6934 (9)	0.628 (2)	0.017 (3)
H2A	0.5789 (8)	0.7721 (9)	0.199 (2)	0.017 (2)
H2B	0.4571 (7)	0.7511 (9)	0.251 (2)	0.016 (2)
H3A	0.5772 (7)	0.7242 (9)	0.805 (2)	0.018 (3)
H3B	0.4584 (7)	0.6826 (10)	0.748 (2)	0.018 (2)

H4A	0.3879 (7)	0.5493 (9)	0.304 (2)	0.017 (2)
H4B	0.4068 (8)	0.4717 (9)	0.481 (2)	0.020 (3)
H5A	0.6362 (7)	0.3931 (9)	0.526 (2)	0.019 (3)
H5B	0.5863 (8)	0.4406 (9)	0.721 (2)	0.018 (2)
H6A	0.7205 (7)	0.5302 (10)	0.170 (3)	0.026 (3)
H6B	0.5992 (8)	0.4994 (10)	0.104 (2)	0.019 (3)
H7A	0.4395 (7)	0.4789 (9)	0.953 (2)	0.021 (3)
H7B	0.4843 (8)	0.3642 (9)	0.998 (3)	0.023 (3)

Atomic displacement parameters (Å²)

	U^{11}	U^{22}	U^{33}	U^{12}	U^{13}	U^{23}
Se1	0.0004 (7)	0.0005 (10)	0.0006 (18)	-0.0001 (7)	-0.0003 (10)	-0.0002 (15)
O1	0.0057 (12)	0.0042 (19)	0.004 (3)	-0.0009 (12)	-0.0004 (16)	-0.0005 (19)
O2	0.0013 (10)	0.0051 (18)	0.005 (3)	-0.0001 (11)	0.0015 (14)	0.002 (2)
O3	0.0041 (13)	0.0042 (19)	0.001 (3)	-0.0006 (11)	0.0013 (15)	-0.0011 (19)
O4	0.0046 (13)	0.0025 (18)	0.004 (3)	0.0004 (12)	0.0005 (15)	0.0016 (19)
Mg1	0.0027 (12)	0.0021 (17)	0.003 (3)	0.0008 (11)	-0.0005 (14)	-0.0019 (19)
OW1	0.0046 (12)	0.008 (2)	0.003 (3)	-0.0021 (12)	0.0007 (17)	-0.001 (3)
OW2	0.0038 (12)	0.0028 (19)	0.007 (3)	0.0004 (11)	-0.0016 (16)	0.000 (2)
OW3	0.0038 (11)	0.007 (2)	0.005 (3)	-0.0004 (13)	0.0005 (15)	-0.001 (2)
OW4	0.0042 (13)	0.006 (2)	0.005 (3)	-0.0011 (13)	-0.0017 (14)	0.000 (2)
OW5	0.0057 (13)	0.0010 (19)	0.006 (3)	0.0000 (12)	0.0002 (14)	0.001 (2)
OW6	0.0046 (13)	0.006 (2)	0.007 (3)	-0.0001 (13)	0.0006 (16)	-0.002 (2)
OW7	0.0064 (14)	0.0040 (19)	0.004 (3)	0.0009 (12)	0.0009 (15)	0.000 (2)
H1A	0.022 (4)	0.020 (5)	0.016 (7)	-0.005 (3)	-0.004 (4)	-0.002 (5)
H1B	0.020 (4)	0.019 (5)	0.013 (8)	-0.006 (3)	-0.004 (4)	-0.002 (5)
H2A	0.019 (4)	0.014 (4)	0.018 (7)	-0.002 (3)	0.007 (4)	0.004 (5)
H2B	0.013 (3)	0.017 (4)	0.018 (7)	0.001 (3)	0.000 (3)	-0.003 (5)
H3A	0.015 (3)	0.019 (5)	0.019 (7)	-0.003 (3)	0.001 (4)	-0.012 (5)
H3B	0.009 (3)	0.024 (5)	0.021 (7)	0.001 (3)	0.005 (3)	-0.002 (5)
H4A	0.016 (3)	0.021 (5)	0.013 (7)	0.001 (3)	-0.006 (3)	-0.002 (5)
H4B	0.022 (4)	0.016 (4)	0.021 (8)	-0.007 (3)	-0.001 (4)	0.005 (5)
H5A	0.021 (3)	0.014 (4)	0.021 (8)	0.002 (3)	0.003 (4)	-0.004 (5)
H5B	0.020 (4)	0.022 (5)	0.011 (7)	-0.001 (3)	0.002 (4)	0.001 (5)
H6A	0.009 (3)	0.030 (6)	0.039 (10)	0.002 (3)	0.004 (4)	0.001 (6)
H6B	0.018 (3)	0.023 (5)	0.015 (8)	-0.005 (3)	-0.002 (4)	-0.004 (5)
H7A	0.015 (3)	0.018 (5)	0.030 (9)	0.007 (3)	0.001 (4)	0.007 (5)
H7B	0.026 (4)	0.016 (5)	0.028 (9)	-0.003 (3)	-0.002 (5)	0.013 (6)

Geometric parameters (Å, °)

Se1—O1	1.630 (6)	OW2—H2A	0.983 (14)
Se1—O3	1.631 (8)	OW2—H2B	0.984 (11)
Se1—O2	1.642 (4)	OW3—H3A	0.976 (13)
Se1—O4	1.661 (7)	OW3—H3B	0.985 (9)
Mg1—OW4	2.037 (6)	OW4—H4B	0.964 (13)
Mg1—OW1	2.045 (6)	OW4—H4A	0.976 (14)

Mg1—OW3	2.046 (10)	OW5—H5B	0.967 (15)
Mg1—OW6	2.058 (9)	OW5—H5A	0.976 (14)
Mg1—OW5	2.097 (8)	OW6—H6A	0.976 (10)
Mg1—OW2	2.104 (8)	OW6—H6B	0.982 (14)
OW1—H1B	0.968 (16)	OW7—H7B	0.955 (13)
OW1—H1A	0.969 (16)	OW7—H7A	0.973 (10)
O1—Se1—O3	109.7 (3)	OW5—Mg1—OW2	177.3 (3)
O1—Se1—O2	110.5 (3)	H1B—OW1—H1A	107.8 (12)
O3—Se1—O2	110.8 (4)	H1B—OW1—Mg1	124.8 (9)
O1—Se1—O4	109.8 (4)	H1A—OW1—Mg1	119.5 (9)
O3—Se1—O4	107.4 (3)	H2A—OW2—H2B	104.2 (12)
O2—Se1—O4	108.6 (3)	H2A—OW2—Mg1	115.9 (7)
OW4—Mg1—OW1	179.2 (5)	H2B—OW2—Mg1	121.0 (7)
OW4—Mg1—OW3	90.3 (3)	H3A—OW3—H3B	108.0 (11)
OW1—Mg1—OW3	88.9 (4)	H3A—OW3—Mg1	127.8 (8)
OW4—Mg1—OW6	93.7 (3)	H3B—OW3—Mg1	118.5 (10)
OW1—Mg1—OW6	87.2 (3)	H4B—OW4—H4A	105.5 (11)
OW3—Mg1—OW6	175.7 (3)	H4B—OW4—Mg1	124.4 (8)
OW4—Mg1—OW5	89.3 (3)	H4A—OW4—Mg1	124.5 (8)
OW1—Mg1—OW5	90.9 (3)	H5B—OW5—H5A	107.7 (11)
OW3—Mg1—OW5	89.0 (4)	H5B—OW5—Mg1	115.3 (7)
OW6—Mg1—OW5	89.4 (3)	H5A—OW5—Mg1	115.3 (10)
OW4—Mg1—OW2	88.1 (3)	H6A—OW6—H6B	109.0 (13)
OW1—Mg1—OW2	91.7 (3)	H6A—OW6—Mg1	125.2 (11)
OW3—Mg1—OW2	91.7 (3)	H6B—OW6—Mg1	125.1 (8)
OW6—Mg1—OW2	90.0 (4)	H7B—OW7—H7A	103.7 (11)

Hydrogen-bond geometry (\AA , $^\circ$)

$D-H\cdots A$	$D-H$	$H\cdots A$	$D\cdots A$	$D-H\cdots A$
OW1—H1A \cdots O3 ⁱ	0.969 (16)	1.692 (16)	2.659 (9)	175.4 (13)
OW1—H1B \cdots O4 ⁱⁱ	0.968 (16)	1.757 (15)	2.724 (9)	175.1 (11)
OW2—H2A \cdots O2 ⁱ	0.983 (14)	1.781 (15)	2.757 (9)	171.0 (11)
OW2—H2B \cdots O4 ⁱⁱⁱ	0.984 (11)	1.753 (11)	2.732 (7)	172.4 (10)
OW3—H3A \cdots O2 ⁱⁱ	0.976 (13)	1.889 (13)	2.861 (8)	174.5 (12)
OW3—H3B \cdots O3 ^{iv}	0.985 (9)	1.708 (9)	2.692 (6)	177.4 (14)
OW4—H4A \cdots O1 ⁱⁱⁱ	0.976 (14)	1.720 (15)	2.688 (9)	170.9 (11)
OW4—H4B \cdots O2 ^v	0.964 (13)	1.927 (11)	2.861 (7)	162.3 (15)
OW5—H5A \cdots O4	0.976 (14)	1.874 (14)	2.839 (8)	169.6 (10)
OW5—H5B \cdots OW7	0.967 (15)	1.786 (14)	2.742 (9)	169.4 (10)
OW6—H6A \cdots OW5 ⁱ	0.976 (10)	1.875 (10)	2.841 (6)	170.3 (12)
OW6—H6B \cdots OW7 ^{vi}	0.982 (14)	1.809 (13)	2.787 (8)	173.4 (11)
OW7—H7A \cdots O1 ^{iv}	0.973 (10)	1.858 (12)	2.790 (7)	159.5 (14)
OW7—H7B \cdots OW2 ^{vii}	0.955 (13)	1.946 (16)	2.866 (8)	161.2 (15)

Symmetry codes: (i) $-x+3/2, -y+1, z-1/2$; (ii) $-x+3/2, -y+1, z+1/2$; (iii) $-x+1, y+1/2, -z+1/2$; (iv) $-x+1, y+1/2, -z+3/2$; (v) $x-1/2, -y+1/2, -z+1$; (vi) $x, y, z-1$; (vii) $-x+1, y-1/2, -z+3/2$.